NAVAL POSTGRADUATE SCHOOL
Monterey, California

THESIS

ANALYSIS OF UNDERBEAD CRACKING IN UNDERWATER WET WELDMENTS ON A516 GRADE 70 STEEL
by
Ryan D. Manning
September 1998
Thesis Advisor: Alan G. Fox

Approved for public release; distribution is unlimited.

REPORT DOCUMENTATION PAGE

Public reporting burden for this collection of information is estimated to average 1 hour per response, including the time for reviewing instruction, searching existing data sources, gathering and maintaining the data needed, and completing and reviewing the collection of information. Send comments regarding this burden estimate or any other aspect of this collection of information, including suggestions for reducing this burden, to Washington headquarters Services, Directorate for Information Operations and Reports, 1215 Jefferson Davis Highway, Suite 1204, Arlington, VA 22202-4302, and to the Office of Management and Budget, Paperwork Reduction Project (0704-0188) Washington DC 20503.

1. AGENCY USE ONLY *(Leave blank)*	2. REPORT DATE September 1998	3. REPORT TYPE AND DATES COVERED Master's Thesis

4. TITLE AND SUBTITLE ANALYSIS OF UNDERBEAD CRACKING IN UNDERWATER WET WELDMENTS ON A516 GRADE 70 STEEL	5. FUNDING NUMBERS
6. AUTHOR(S) Manning, Ryan D.	

7. PERFORMING ORGANIZATION NAME(S) AND ADDRESS(ES) Naval Postgraduate School Monterey, CA 93943-5000	8. PERFORMING ORGANIZATION REPORT NUMBER

9. SPONSORING / MONITORING AGENCY NAME(S) AND ADDRESS(ES) Naval Sea Systems Command (NAVSEA OOC) 2531 Jefferson Davis Hwy Arlington, VA 22242--5160	10. SPONSORING / MONITORING AGENCY REPORT NUMBER

11. SUPPLEMENTARY NOTES
The views expressed in this thesis are those of the author and do not reflect the official policy or position of the Department of Defense or the U.S. Government.

12a. DISTRIBUTION / AVAILABILITY STATEMENT Approved for public release; distribution is unlimited.	12b. DISTRIBUTION CODE

13. ABSTRACT *(maximum 200 words)*

The use of underwater weldments on US Naval Vessels is highly desirable due to the ability of performing repairs without costly dry dock expenses. The primary problem with underwater wet weldments is underbead cracking in the heat affected zone (HAZ). The fundamental factors causing underbead cracking in underwater wet weldments using a shielded metal arc welding (SMAW) process are high quench rates, slag inclusions, diffusable hydrogen levels and porosity.

The weld metal analysis included use of optical and scanning microscopy as well as microhardness testing. Three weld samples made at 5°C, 12°C, and 25°C water temperature were analyzed in this thesis. HAZ underbead cracking was present in all three welds analyzed although the 5°C sample was the only weld that exhibited extensive cracking whereas the 25°C sample only had cracking near the upper 50% of the weld passes. Crack origination in all three samples near the cap was evident and was most likely due to small levels of bead tempering at this location.

This thesis addresses the mechanisms of the cracking as well as the effects of diffusable hydrogen, cooling rates, and water temperatures on wet weldments.

14. SUBJECT TERMS Underwater wet welding, Hydrogen cracking, underbead cracking, Non-metallic inclusions, Shielded Metal Arc Welding	15. NUMBER OF PAGES 50
	16. PRICE CODE

17. SECURITY CLASSIFICATION OF REPORT Unclassified	18. SECURITY CLASSIFICATION OF THIS PAGE Unclassified	19. SECURITY CLASSIFI- CATION OF ABSTRACT Unclassified	20. LIMITATION OF ABSTRACT UL

ANALYSIS OF UNDERBEAD CRACKING IN UNDERWATER WET WELDMENTS ON A516 GRADE 70 STEEL

Ryan Daniel Manning
Lieutenant junior grade, United States Coast Guard
B.S. Civil Engineering, United States Coast Guard Academy, 1994

Submitted in partial fulfillment of the
requirements for the degree of

MASTER OF SCIENCE IN MECHANICAL ENGINEERING

from the

NAVAL POSTGRADUATE SCHOOL
September 1998

ABSTRACT

The use of underwater weldments on US Naval Vessels is highly desirable due to the ability of performing repairs without costly dry dock expenses. The primary problem with underwater wet weldments is underbead cracking in the heat affected zone (HAZ). The fundamental factors causing underbead cracking in underwater wet weldments using a shielded metal arc welding (SMAW) process are high quench rates, slag inclusions, diffusible hydrogen levels and porosity.

The weld metal analysis included use of optical and scanning microscopy as well as microhardness testing. Three weld samples made at 5°C, 12°C, and 25°C water temperature were analyzed in this thesis. HAZ underbead cracking was present in all three welds analyzed although the 5°C sample was the only weld that exhibited extensive cracking whereas the 25°C sample only had cracking near the upper 50% of the weld passes. Crack origination in all three samples near the cap was evident and was most likely due to small levels of bead tempering at this location.

This thesis addresses the mechanisms of the cracking as well as the effects of diffusible hydrogen, cooling rates, and water temperatures on wet weldments.

TABLE OF CONTENTS

ACKNOWLEDGMENT

I would like to express my sincere gratitude and appreciation to Professor Alan G. Fox for his advice, support, patience and motivation throughout the thesis research. I would also like to thank Professor Sarath K. Menon and Mr. Richard Hashimoto for the contribution of their time and and instruction in the laboratory during this thesis research.

I also would like to thank my father and mother who recently passed away for all the love and caring shown over the past years which has given me the motivation to complete this graduate coursework.

I. INTRODUCTION

The use of underwater wet welding is of particular interest to the U.S. Navy because of the money that can be saved by avoiding unnecessary dry docking and the ability to extend time between major overhauls. Because of changes in the specification for underwater welding [Ref. 1], the technique of wet welding has become a possibility. The major problem with this process is the amount of underbead cracking that can occur when welding high strength steels underwater. Because of rapid cooling rates, dissociated hydrogen from the water environment, and the brittle microstructure found in the HAZ of underwater wet weldments, this process is a very difficult one.

Recent research has shown hydrogen assisted underbead cracking in ASTM A516 Grade 70 steel [Ref. 8, 9] over a range of water temperatures. This work indicates that cracking is reduced with increased water temperature. The current research extends this study with refined experimental procedures so that more conclusive information can be gained concerning the understanding of this hydrogen assisted underbead cracking.

II. BACKGROUND

A. UNDERWATER WELDING

Underwater welding is classified by wet or dry processes by the American Welding Society in The Specifications for Underwater Welding. Wet welding processes are made in which the welder and associated work are in direct contact with the underwater environment. Dry welding processes on the other hand are made when the work is protected from the water. The Specifications for Underwater Welding [Ref. 1] outline five underwater welding processes currently in use.

*One Atmosphere Welding - This type of welding is performed within a pressure vessel which is maintained at approximately one atmosphere. The advantage of this process is that the welder does not need diving qualifications as they may be transferred to the pressure vessel to perform the work. This process is also the only underwater welding process which is not performed in a hyperbaric condition, meaning pressure greater than one atmosphere.

*Habitat Welding – This process parallels the one atmosphere process in that the welder does not need to wear their diving gear while performing the weld. Unlike one atmosphere welding, habitat welding is performed at ambient pressure. Because the welder is not in diving gear in either one atmosphere or habitat welding, the chamber must be atmosphere conditioned via a ventilation system.

*Dry Chamber Welding – This process is performed with the welder in diving gear in an open bottom enclosure. Because the diver is being supplied breathing capabilities by his gear, the only need for atmosphere controlling equipment is exhaust of welding and diver gases.

*Dry Spot Welding – This process is performed in which the only the dry area is the space surrounding the actual weld. This area is kept dry via a gas filled box or shielding gas surrounded by a concentric ring of water jets.

*Underwater Wet Welding – This process is performed with the welder striking the arc in the water and performing all work with no separation from weld joint and the water. The shielded metal arc welding (SMAW) that was performed for the work in this thesis utilized this underwater wet welding process.

1.   Underwater Wet vs. Dry Hyperbaric Welding

Because of the costs involved in dry hyperbaric welding processes, underwater wet welding would seem to be the obvious choice of process wherever possible. In addition to being expensive, dry welding processes are limited by their respective pressure vessels and habitats which make them desirable. Because of the thickness of most underwater structures, a high deposition rate is normally required for underwater repairs. The shielded metal arc welding process that is used in the underwater wet welding process usually has a higher deposition rate than gas tungsten arc welding (GTAW) and gas metal arc welding (GMAW) which cannot be performed in wet conditions. Because of the controlled atmosphere that can be maintained in dry hyperbaric welding processes, a variety of welding processes are made possible such as GMAW or GTAW but since their deposition rates do not match the SMAW process they are more time consuming, and therefore more costly. However GMAW and GTAW performed in dry conditions produce a considerably cleaner weld than SMAW. As a result the obvious disadvantage of SMAW is the poorer quality of the resulting weld. The reasons for poor quality have to do with multiple environmental factors such as:

*High cooling rates due to quenching from the surrounding water. The ability to pre and post-heat in underwater wet welds is not available like in dry hyperbaric welds.

*Hydrogen control in the weld area. Because of the direct contact with water, hydrogen is obviously always present around the weld pool. In dry hyperbaric weld processes the environment can be controlled much better.

*Arc stability at depth. Dry hyperbaric welds can maintain a stable arc at great depth.

*Poor visibility of the weld area due to the lack of exhaust gas evacuation systems like those used in dry hyperbaric weld processes.

It seems that all of these environmental factors would prevent the wide use of underwater wet welds and favor dry hyperbaric processes. Of course they do, but the economic gains associated with underwater wet welding using the SMAW process will be the method of choice where possible.

B.   UNDERWATER WET SHIELDED METAL ARC WELDING

As discussed above, the process most commonly used for wet weldments is the shielded metal arc process [Ref. 4]. The base metal used in underwater SMAW must be mindfully selected and the electrodes must be prepared so as to limit water absorption. The welder/diver is obviously restricted in his movements by the required safety gear that he must wear. In addition, the electrical safety of the welder/diver must be of top priority so that injury is not sustained during the welding process. The U.S. Navy Underwater Cutting and Welding Manual shows a typical layout of equipment used for underwater welding operations [Ref. 5]. This equipment is shown in Figure 2.1. Underwater shielded metal arc welding is very similar to the SMAW process performed in air. Major

differences include, electrodes with special fluxes and waterproof coating so as to minimize hydrogen absorption, direct current straight polarity for the safety of the welder/diver, and welding/safety equipment remote to the work. Otherwise the process is very similar to that shown in Figure 2.2 [Ref. 6].

C. THE HEAT AFFECTED ZONE MICROSTRUCTURE OF UNDERWATER WET WELDS MADE ON FERRITIC STEEL

Rapid cooling rates in underwater wet welds have a direct affect on the microstructure surrounding the weld metal. Martensite microstructures are very common during the underwater welding of ferritic steels as well as porosity within the weld metal due to the rapid cooling and subsequent solidification of the weld metal. One of the most undesirable consequences of underwater wet welding is the dissociation of water by the weld arc which leads to increased hydrogen levels in the weld pool and thus in the heat affected zone near the fusion line. This increase of hydrogen in the HAZ combined with a martensitic microstructure leaves the weld susceptible to underbead cracking. In order to minimize the amount of martensite formed due to these rapid cooling rates the carbon equivalent (CE) of the base metal to be welded has been set at a maximum of 0.40 wt % [Ref. 1]. A possible solution when welding steels with a higher CE than 0.40 wt % is to use austenitic weld metals. Austenitic weld metals have two properties which help reduce underbead cracking [Ref. 6]. Austenite has a much higher ability than α ferrite to dissolve hydrogen and, because of the increased ductility of austenitic weld metal, the high stresses associated with underbead cracking can be relieved.

1. Material Selection

An equation for finding the carbon equivalent of weld metals has been presented in the *Specification for Underwater Welding* [Ref. 1]. Because this number is of utmost

importance it must be calculated for materials selected for the underwater SMAW process.

$$CE = C + (Mn / 6) + ((Cr + V + Mo) / 5) + ((Cu + Ni) / 15)$$

$CE = Carbon\ Equivalent$

$C = Weight\ \%\ Carbon$

$Mn = Weight\ \%\ Manganese$

$Cr = Weight\ \%\ Chromium$

$V = Weight\ \%\ Vanadium$

$Mo = Weight\ \%\ Molybdenum$

$Cu = Weight\ \%\ Copper$

$Ni = Weight\ \%\ Nickel$

A careful selection of the base metal and weld metal must consider a comparison of CE. If the same strength is desired in the fusion zone as found in the base plate the CE would be similarly matched, but the weld metal commonly has a lower CE than the base plate in order that it is more ductile so that cracking is avoided. For example, the carbon content of the E7014 type electrode used in the present work is around 0.006 wt% with a CE of about 0.17. In research done by Masubuchi, et al [Ref. 7] on the underwater welding of ferritic steels hydrogen underbead cracking did occur in ferritic steels with CEs in the range 0.30 to 0.42. In the current research the base metal studied (ASTM A516 Grade 70) has a CE of 0.39 with a C content of 0.20 wt %.

2.   Rapid Cooling Rate

As discussed previously, the weld microstructure is affected by the rapid cooling rates incurred in underwater welding. The use of a continuous cooling transformation

(CCT) diagram can explain this microstructure. Figure 2.3 is a CCT of simulated single pass welds on A516 Gr 70 steel which was generated using a Gleeble machine. The microstructures and corresponding temperatures at which each will start and finish can be identified on the diagram. Because the weld samples of interest were multipass welds, an important variable known as bead tempering is introduced. Lundin, et al [Ref. 3] explain the role of subsequent weld passes and its affect on the previous weld pass microstructure. Figure 2.4 shows how multiple weld passes can affect the HAZ of the weld pass made previous to it. Multiple weld passes provide bead tempering to the previous weld pass which refines the coarse grains in the HAZ which is where hydrogen underbead cracking commonly exists. In research performed by Fox, et al [ref. 8] the time for the HAZ at the fusion line to cool from 800°C to 500°C (Δt_{8-5}) in wet welds made in 3°C and 31°C water were very similar at 1.15-1.2 seconds. Figure 2.3 indicates that this cooling time is associated with predominately martensitic microstructure.

3.   Hydrogen Cracking

The susceptibility to hydrogen cracking in underwater weldments made on high strength steels is a major concern. Kou [Ref. 6] explains the four conditions which must be present for hydrogen cracking to occur:

1) Susceptible microstructure

2) Critical concentration of diffusible hydrogen

3) Stress intensity

4) Relatively low temperature less than 200°C

As can be expected, all four conditions exist in underwater SMAW. Obviously the martensitic microstructure of the HAZ near the fusion line is susceptible because it is

hard and brittle. The dissociation of hydrogen near the weld arc unavoidably supplies

hydrogen to the weld metal. Because of the high restraints placed on the weld piece and

the superimposing of large thermal gradients, high stresses are likely in the weld.

Finally, the temperature of any underwater body that is available for work to be

accomplished in is definitely below 200°C. The comments made in all the subsections of

section C clearly indicate that hydrogen assisted underbead cracking of underwater wet

weldments on ferritic steel is highly likely unless the steel's carbon equivalent and carbon

contents are maintained at suitably low levels.

D.   SCOPE OF THE PRESENT WORK

The ability to weld high strength steels underwater is of great importance to the

U.S. Navy. Previous research governing the effects of water temperature on the

underwater wet weldability of ASTM A516 Grade 70 steel has been performed at the

Naval Postgraduate School. The thesis research of LT Robert L. Johnson was conducted

on three different underwater weld samples made in 3°C, 10°C and 31°C water. The 3°C

and 10°C weld samples were made in seawater and the 31°C sample was made in a

freshwater test tank. In addition, the depth of water at which the samples were welded

varied from 5.5 to 7.3 meters. This research is an extension of the previous research

which attempts to have a more strict control on weld parameters so as to eliminate

possible differences such as water depth and type and welding heat input. All three weld

samples were performed at the same depth of 8.2 meters in a fresh water test tank. In

addition, the weld power was very similar for all three weld samples. The objectives of

determining the cause and mechanisms of cracking as well as determining the effect of

water temperature on the weld metal and HAZ in ASTM A516 Grade 70 steels are still

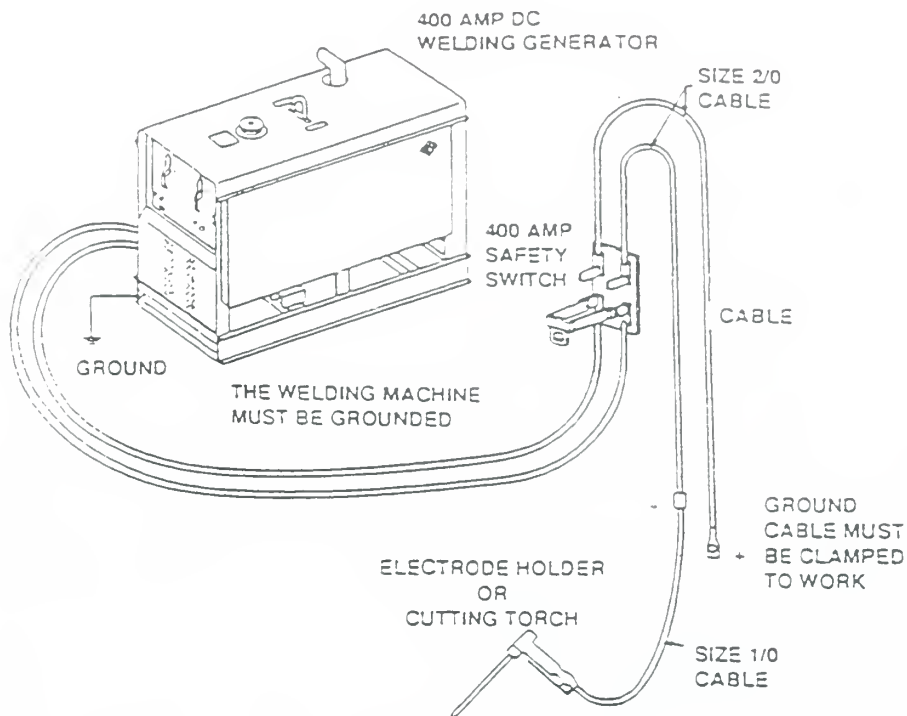the primary goals for the research.

Figure 2.1 Welding and safety equipment configuration for Underwater welding and cutting [Ref. 5]
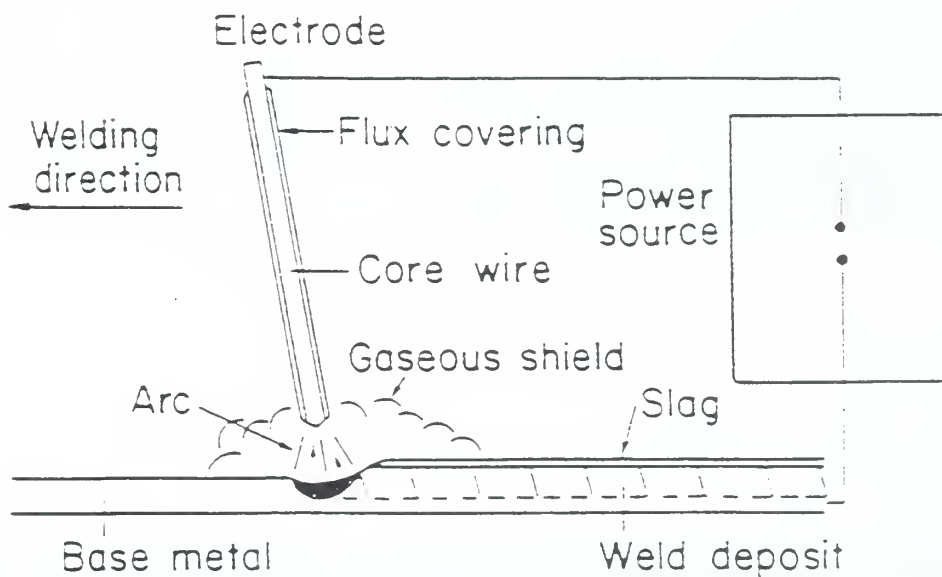

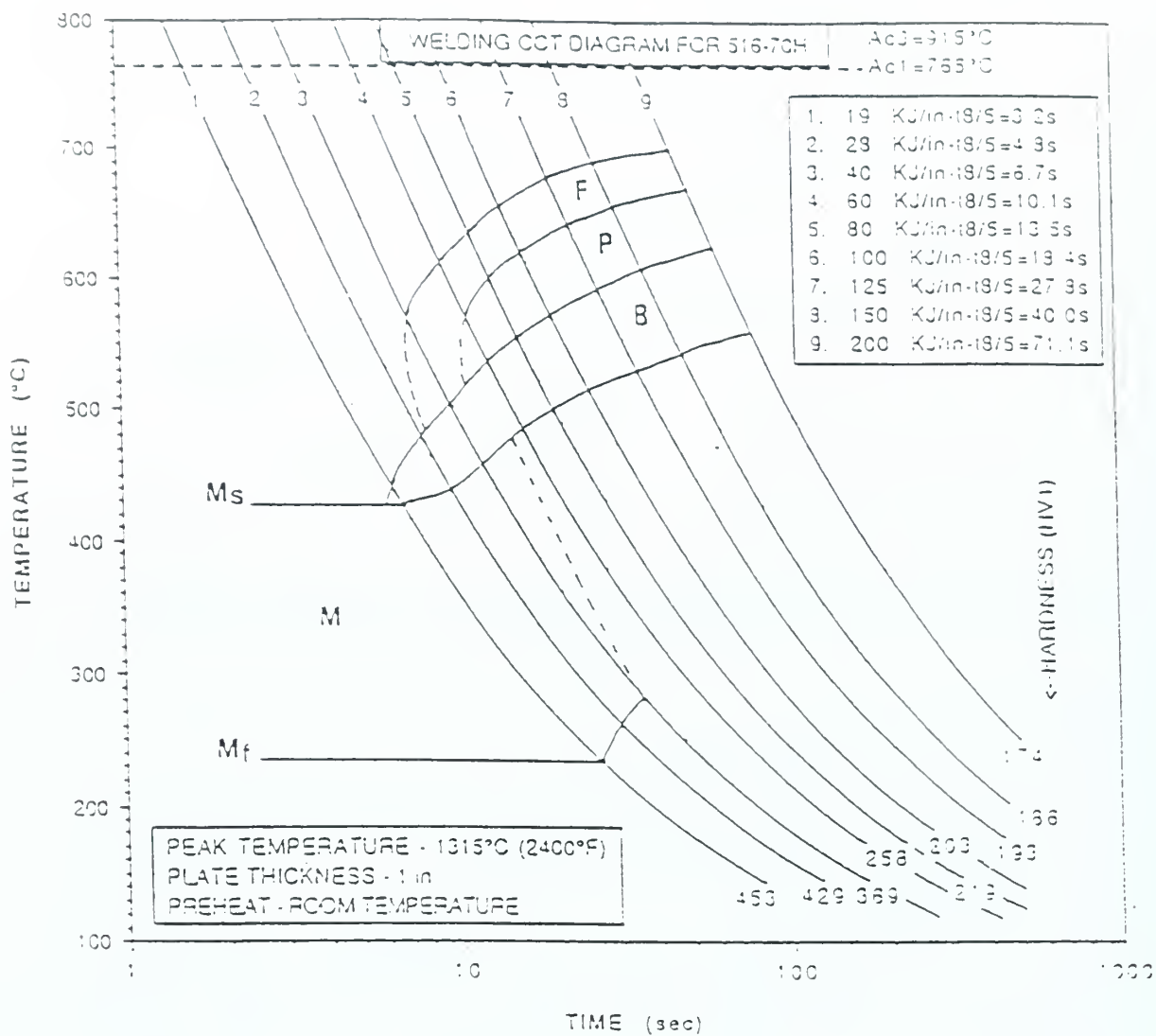Figure 2.2 Sketch of the shielded metal arc welding process [Ref. 6]

11

Figure 2.3 Continuous Cooling Transformation diagram for a single pass weld on A516 Grade 70 Steel [Ref. 3]
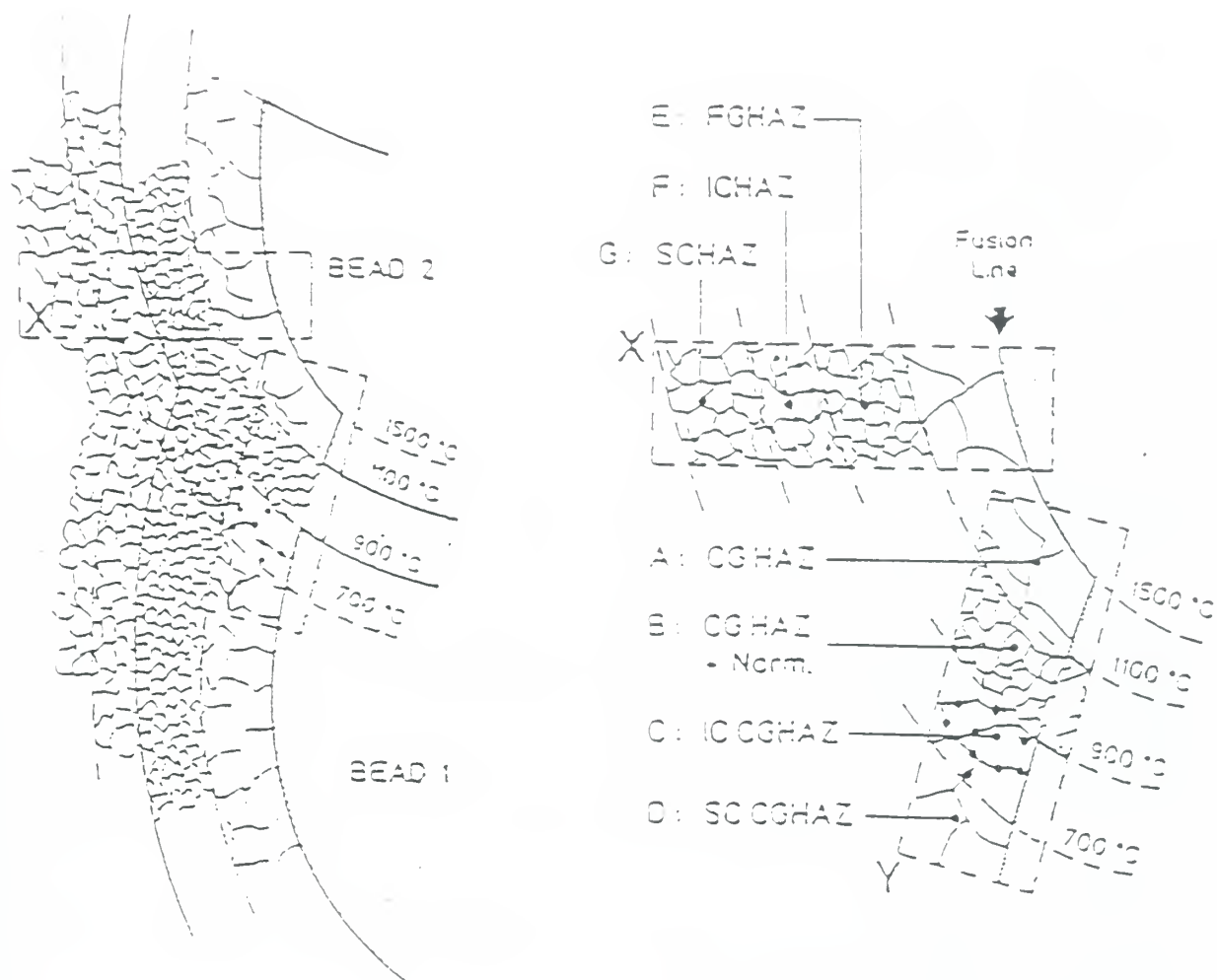
Figure 2.4 Schematic diagram of the multipass weld HAZ microstructure [Ref. 3]

III. EXPERIMENTAL METHODS

A.   WELD SAMPLES

Three shielded metal arc weldments made on ASTM A516 Grade 70 steel in 5°C, 12°C, and 25°C water were received from NAVSEA (OOC5) for analysis. The welds samples will be referred to as UWW05, UWW12, and UWW25 which is short for underwater wet weldment and the corresponding water temperature at which the weld was performed. All welds were performed on 19.05 mm (3/4 in) thick plate of ASTM A516 Grade 70 steel using a 3.175 mm (1/8 in) diameter Broco UW-CS-1 electrode which is an E7014 basic electrode with a waterproof Al_3Si coating. The joint design was B1V.1 for all three weld samples with the plates being fully restrained by strongbacks. The welding experiments were performed in a fresh water test tank at Phoenix Marine in Berwick, LA. Welding parameters and conditions are listed in Table 3.1. The test plates had a carbon equivalent of 0.391 and 0.20 wt % carbon content.

B.   SAMPLE PREPARATION

The three weld samples of 60.96 cm (24 in) in length were shipped to the Naval Postgraduate School for analysis. Sectioning of the weld samples was accomplished using a Powermet 2000 Automatic Abrasive Cutter. The samples were then prepared by wet sanding on a Struers Knuth-Rotor-3 with 180, 320, 500, 1000, 2400, and 4000 Struers waterproof silicon carbide paper followed by fine polishing on the Metaserv 2000 grinder/polisher using 6 micron Buehler Metadi diamond compound aerosol spray and 0.05 µm Buehler micropolish gamma alumina. Scanning electron microscopy was performed on the samples in the polished state after which the samples were etched in a

solution of 5% nital for 10 seconds for optical microscopy. The weld samples were given a final etching in a solution of 5% nital for 2 minutes for macroscopic photographs.

C. SCANNING ELECTRON MICROSCOPY

Two different scanning electron microscopes were used in this thesis research. The Cambridge Stereoscan S200 was used to analyze the fracture surfaces associated with the underbead cracking while the Topcon SM-510 was used to analyze the inclusions. The energy dispersive analysis of emitted x-rays (EDX) detector on the SM-510 was used to identify slag and oxide inclusions. While making the inclusion observations the tungsten filament was energized to 20 KV, the working distance was set to 29 mm, and the magnification was set to 6900X. Fifty fields of each sample were analyzed for number, size, type, and volume fraction. Each of the fifty fields were 2.17×10^{-10} m^2 in size. Figure 3.1 shows a typical inclusion field analyzed. The inclusion data gathered was used to find the size and number of each. Statistical analysis was then performed with this data to find the mean size and standard deviation of each inclusion type.

D. OPTICAL MICROSCOPY

The initial etching previously described was then carried out and optical microscopy was performed on the Carl Zeiss Jena Jenaphot 2000 optical microscope. Semicaps software was used in conjunction with a Pulnix TMC-74 camera to obtain micrographs from the areas of interest on the weld sample. After the deep etching described previously was performed macroscopic photographs were taken by GRM Photo, Inc. using a standard 35 mm camera. The photographs are shown in Figures 3.2 through 3.4.

E.   MICROHARDNESS ANALYSIS

Microhardness measurements were performed on the three weld samples using a Buehler Micromet 2004 microhardness testing machine. A 200 gram load was applied and readings were obtained in Hardness Vickers (HV). Readings were obtained in the heat affected zone (HAZ) near the cap of the final pass as well as around each of the underbead cracks located near the final pass.

Weld Sample #	Welding Conditions and Parameters					
	Temperature	Depth	Location	Weld Position	Weld Rate	Weld Power
UWW05	5C (41F)	8.2 m (27 ft)	Fresh Water	Horizontal	221-269 mm/min	0.94-1.47 kJ/mm
UWW12	12.2C (54F)	8.2 m (27 ft)	Fresh Water	Horizontal	219-302 mm/min	1.04-1.81 kJ/mm
UWW25	25C (77F)	8.2 m (27 ft)	Fresh Water	Horizontal	210-259 mm/min	1.00-1.72 kJ/mm

Table 3.1 Welding conditions and parameters

Figure 3.1 SEM micrograph of typical inclusion field in UWW05
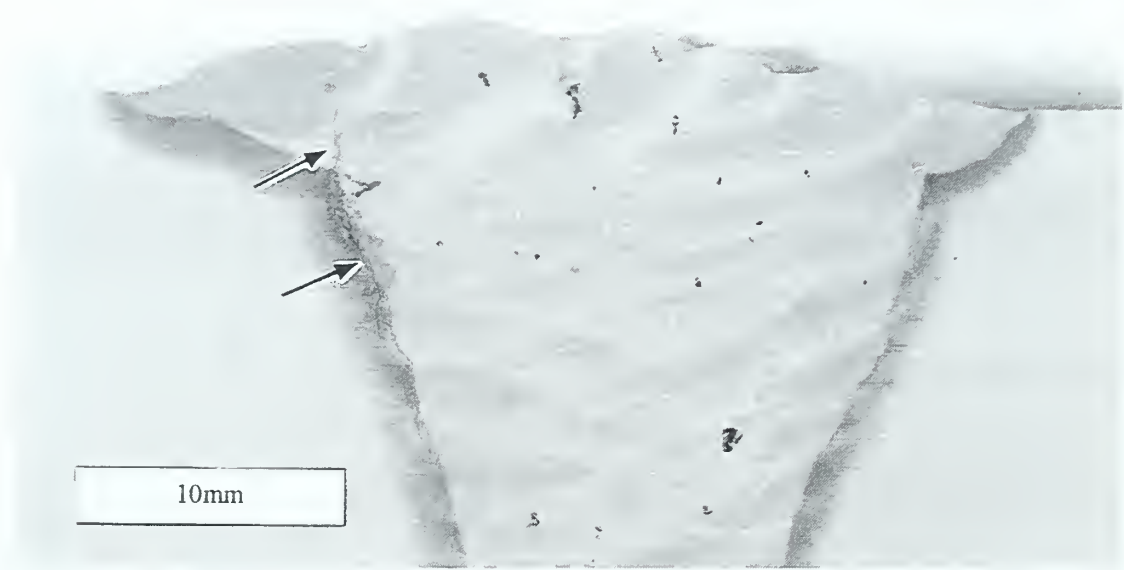
Figure 3.2 Macrophotograph of UWW05 weld sample – Underbead cracks are indicated by arrows
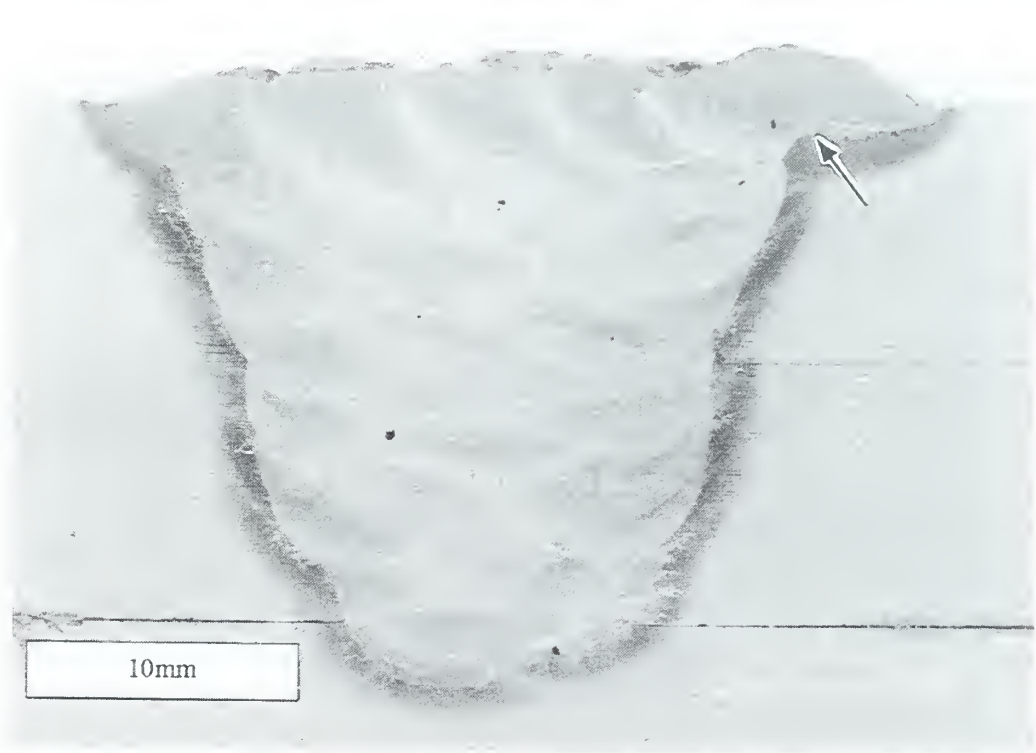
Figure 3.3 Macrophotograph of UWW12 weld sample – Underbead cracking is indicated by an arrow
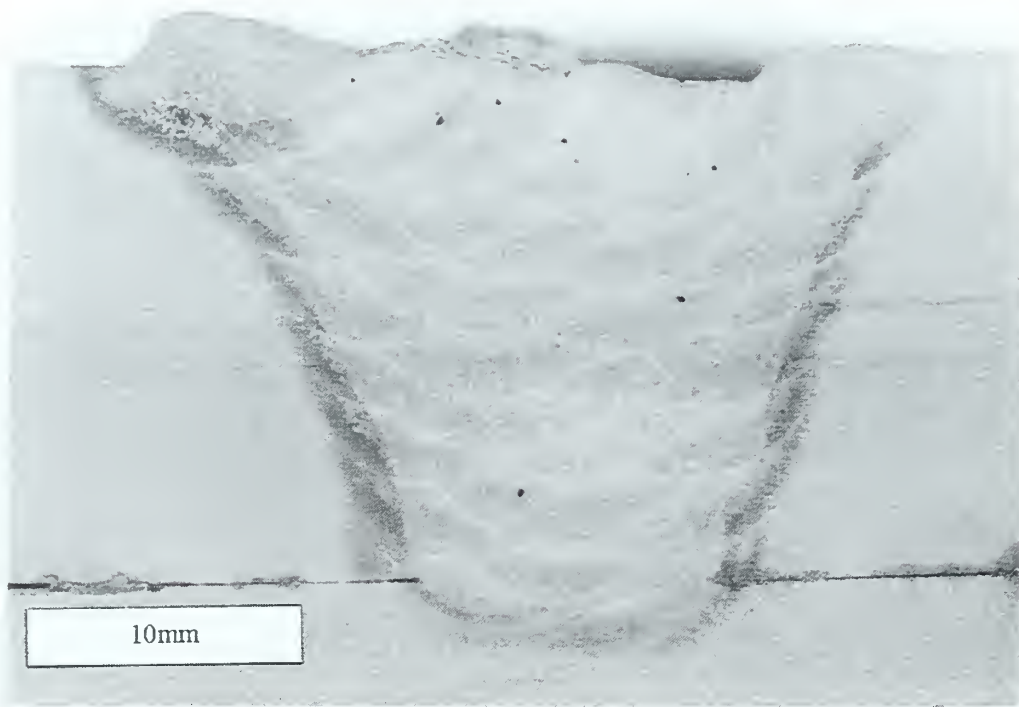
Figure 3.4 Macrophotograph of UWW25 weld sample – Underbead cracks cannot be seen at this magnification

IV. RESULTS AND DISCUSSION

A. NON-METALLIC INCLUSIONS

1. Size and Volume Fraction

The mean size, standard deviation and volume fraction was determined for the inclusions present in each of the fifty fields analyzed in each sample. The typical inclusion field shown in Figure 3.1 would by analyzed by counting, sizing, and identifying each inclusion through the use of the EDX. The results were then tabulated in a spreadsheet for calculation of mean size and number, standard deviation, and confidence. This data is shown in Tables 4.1 – 4.3.

2. Inclusion Microchemical Analysis

An electron probe was placed on each inclusion to identify it as oxide or slag by the use of EDX.. Deoxidation inclusions were normally spherical and showed strong characteristic x-rays of silicon, titanium, and manganese. Slag inclusions on the other hand normally had an irregular shape and showed strong characteristic x-rays of aluminum, as well as smaller signals of silicon and calcium. Figure 4.1 and 4.2 shows typical EDX spectra for deoxidation and slag inclusions respectively. Classification of the smaller inclusions ($< 0.2\mu m$) was somewhat difficult as they did not give an EDX spectrum much different from the weld metal spectrum. The reason for this is that the bulb of interaction of the electron microprobe actually extends far into the weld metal beneath the inclusion. [Ref. 2] This bulb of interaction of the electron microprobe can be seen in Figure 4.3.

B.   MICROHARDNESS ANALYSIS

The microhardness measurements described in the experimental procedure section are listed in Table 4.4. Figure 4.4 shows the typical regions where microhardness measurements were taken. With an average hardness of 296-297 HV in the HAZ near the last pass weld cap area, this is an indication that the microstucture is martensite and bainite as was confirmed by optical microscopy. The average hardness around the cracks found near the last pass of the weld was between 360 and 366 HV. This indicates that the microstructure is nearly all martensite and explains the reason that cracking occurred in this hard and brittle section of the HAZ.

C.   MICROSTRUCTURAL ANALYSIS
1.   Macroscopic

The macroscopic photographs taken by GRM Photo, Inc. that appear as Figures 3.2 -3.4 show various features of the weld samples. At this magnification extensive cracking from the weld cap to the root is seen on the UWW05 sample whereas the cracks in the UWW12 and UWW25 are somewhat localized near the cap of the last weld pass and are much finer. The additional feature that can be seen because of the deep etching is the effects of the multipass weld as described by Lundin, et al., [Ref. 3] and seen in Figure 2.4. Bead tempering is evident in all of the passes except the last one. This suggests a reason why the cracks are likely to originate near the last weld pass because this area of the weld sample has the highest hardness which was confirmed by microhardness measurements.

2.   Microscopic

After an etch in a solution of 5% Nital for 10 seconds the samples were examined in the optical microscope at magnifications of 160X and 320X to determine the

microstructure in which the cracks were found. The cracks nearly always were found in the coarse grain region of the HAZ near the fusion line. The cracks would eventually be arrested after branching into the base metal or into the fine grain region of the HAZ. The extensive crack branching found in UWW05 is shown in the micrographs in Figures 4.5 and 4.6. Note the microstructure in this region is essentially martensite and bainite. In addition, the microstructure of the weld metal was also analyzed to confirm the findings of Fox et al and Murray et al [Ref. 8, 9]. The weld metal microstructure was found to consist mostly of acicular ferrite with smaller amounts of Widmanstatten (side plate) ferrite, grain boundary ferrite, martensite and bainite.

3. Fractography

Underbead crack surfaces of UWW05 were examined in the S200 SEM to determine the mechanism of failure. Transgranular cracking and secondary cracking perpendicular to the fracture surface were clearly seen in this sample. Figure 4.7 is a micrograph which clearly shows these features which are typical of hydrogen assisted cracking.

D. DIFFUSIBLE HYDROGEN LEVELS

The diffusivity of hydrogen in the HAZ is of particular interest. For hydrogen assisted underbead cracking to occur there must be some hydrogen remaining in the coarse grain heat affected zone. According to Fox et al [Ref. 8] the difference in cooling time from 800°C to 100°C between a underwater wet weld made at 3°C and 31°C is less than 10 seconds. While this difference may seem small, a diffusion calculation indicated that the diffusivity of hydrogen was 3.7 times slower in the 3°C sample than the 31°C sample. This diffusivity is calculated given the diffusivity coefficient used by Easterling

[Ref. 10] for temperatures below 200°C. This is $D_o = 1.2 \times 10^{-3}$ cm^{2}s^{-1} with an activation energy of $Q = 3.27 \times 10^4$ Jmol^{-1}. Using these same constants the diffusivity of hydrogen in UWW05 = 8.55×10^{-10} cm^{2}s^{-1} and in UWW25, $D = 2.00 \times 10^{-9}$ cm^{2}s^{-1}. This results in a diffusivity of hydrogen that is 2.6 times slower in UWW05, which could explain the difference in underbead cracking. Figure 4.8 shows the variation in diffusivities of hydrogen with respect to temperature. As can be seen, there is a rapid decline of the diffusivity coefficient around 200°C in ferritic steels together with a large scatterband of values which no doubt arises because of the differing numbers of defects acting as sinks in the different samples studied. This explains our large difference in diffusivity of hydrogen between two temperatures that have such a small temperature differential. Easterling [Ref. 10] explains that this sudden drop is likely due to the increased amount of sinks found in the ferritic steel at temperatures less than 200°C such as inclusions, cracks, and other various defects.

Type	Average Number Incl/Field	Average Diameter μm	Standard Deviation μm	99% Confidence	Volume Fraction %
Oxide	8.8	0.496432	0.274844	0.033739	0.01026
Slag	0.84	1.308929	1.306279	0.519025	0.0104
Total	9.64	0.56723	0.466524	0.054718	0.02066

Table 4.1 Inclusion statistics and volume fraction, UWW05

Type	Average Number Incl/Field	Average Diameter μm	Standard Deviation μm	99% Confidence	Volume Fraction
Oxide	7.86	0.479644	0.293232	0.038088	0.009
Slag	0.58	1.581034	1.552996	0.742589	0.01032
Total	8.44	0.555332	0.495798	0.062148	0.0193

Table 4.2 Inclusion statistics and volume fraction, UWW12

Type	Average Number Incl/Field	Average Diameter μm	Standard Deviation μm	99% Confidence	Volume Fraction
Oxide	9.52	0.481197	0.211558	0.024969	0.00952
Slag	0.52	0.673077	0.305473	0.154263	0.00102
Total	10.04	0.491135	0.21742	0.024988	0.01056

Table 4.3 Inclusion statistics and volume fraction, UWW25

Sample	Crack near cap (HV)	HAZ next to weld cap (HV)
UWW05:		
Max	432	387
Ave	363	296
Min	289	196
UWW12:		
Max	424	397
Ave	360	297
Min	305	208
UWW25:		
Max	440	438
Ave	366	296
Min	240	195

Table 4.4 Weld Sample Vickers Microhardness Data
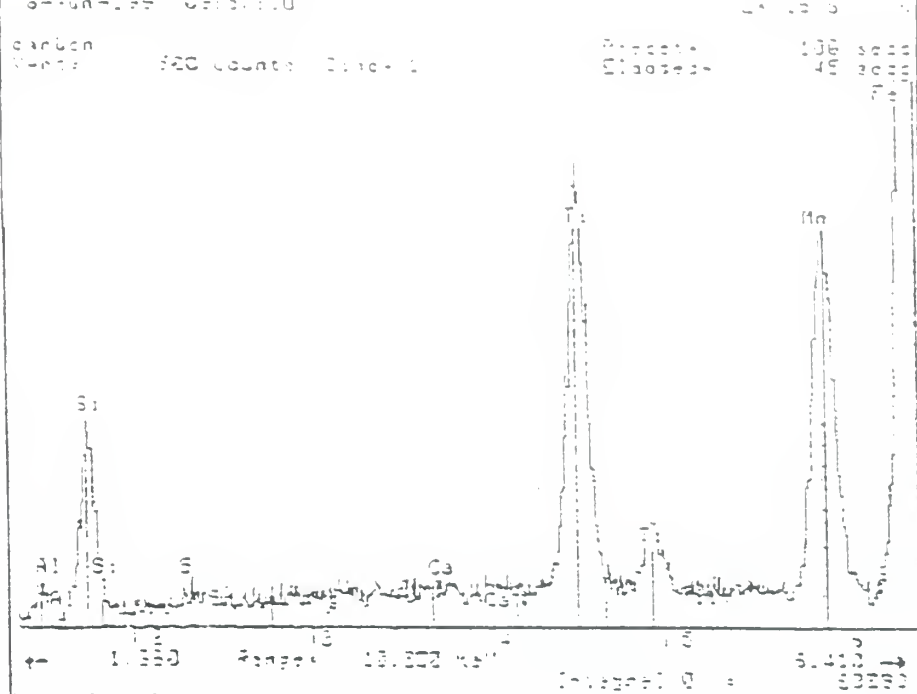
Figure 4.1 Typical Oxide Inclusion EDX Spectrum [Ref. 11]
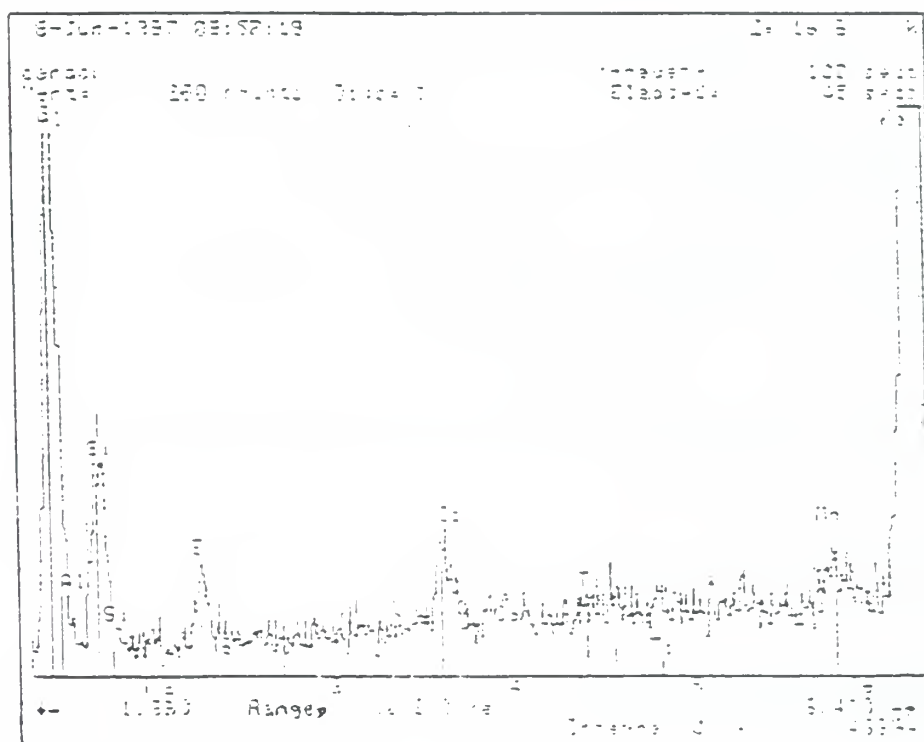
Figure 4.2 Typical Slag Inclusion EDX Spectrum [Ref. 11]
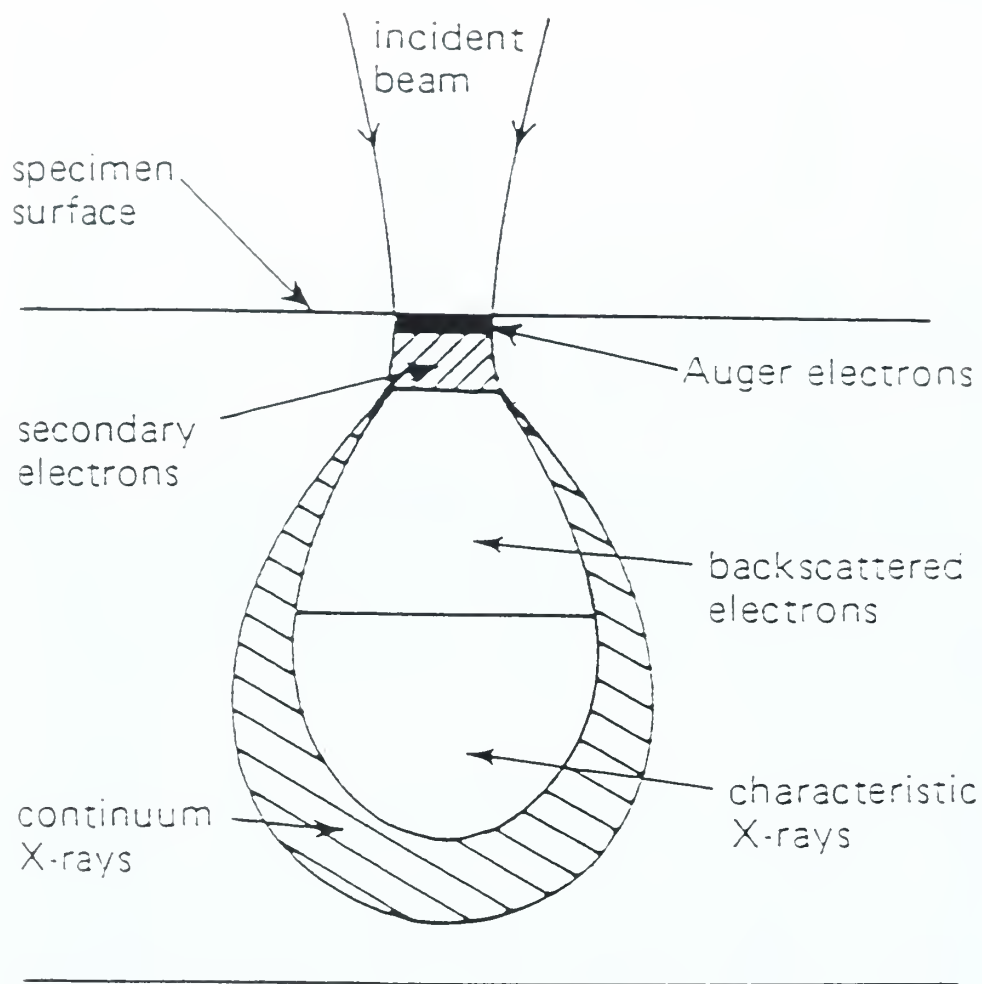
Figure 4.3 Schematic diagram showing generation of electrons and x-rays with in the specimen [Ref. 2]
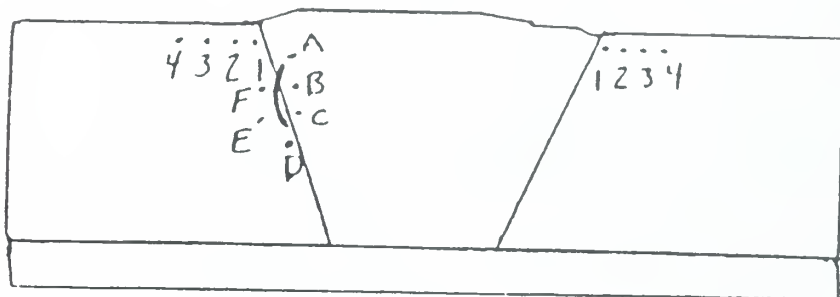
Figure 4.4 Typical regions where microhardness readings were taken
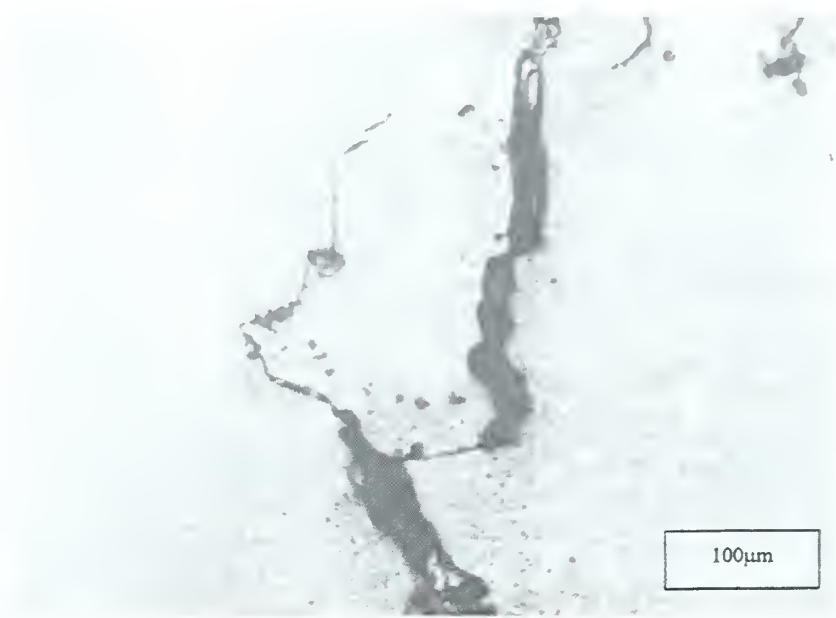
Figure 4.5 Optical micrograph of UWW05 showing extensive crack branching

Figure 4.6 Optical micrograph of UWW05 showing martensite microstructure
surrounding crack
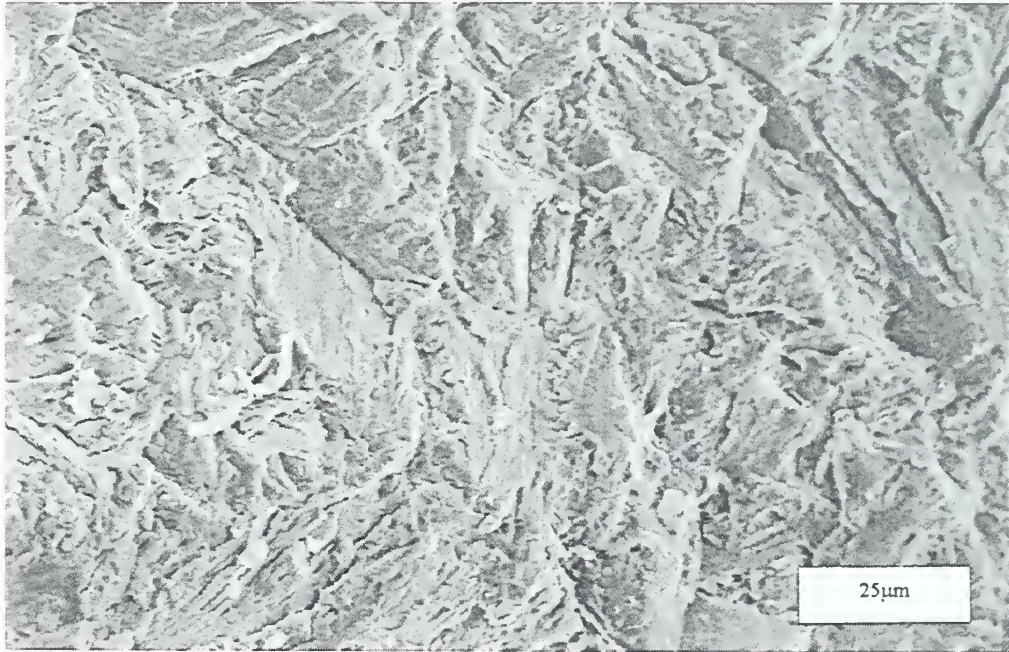
Figure 4.7 SEM micrograph of transgranular cracking on the surface of the fracture with secondary cracking
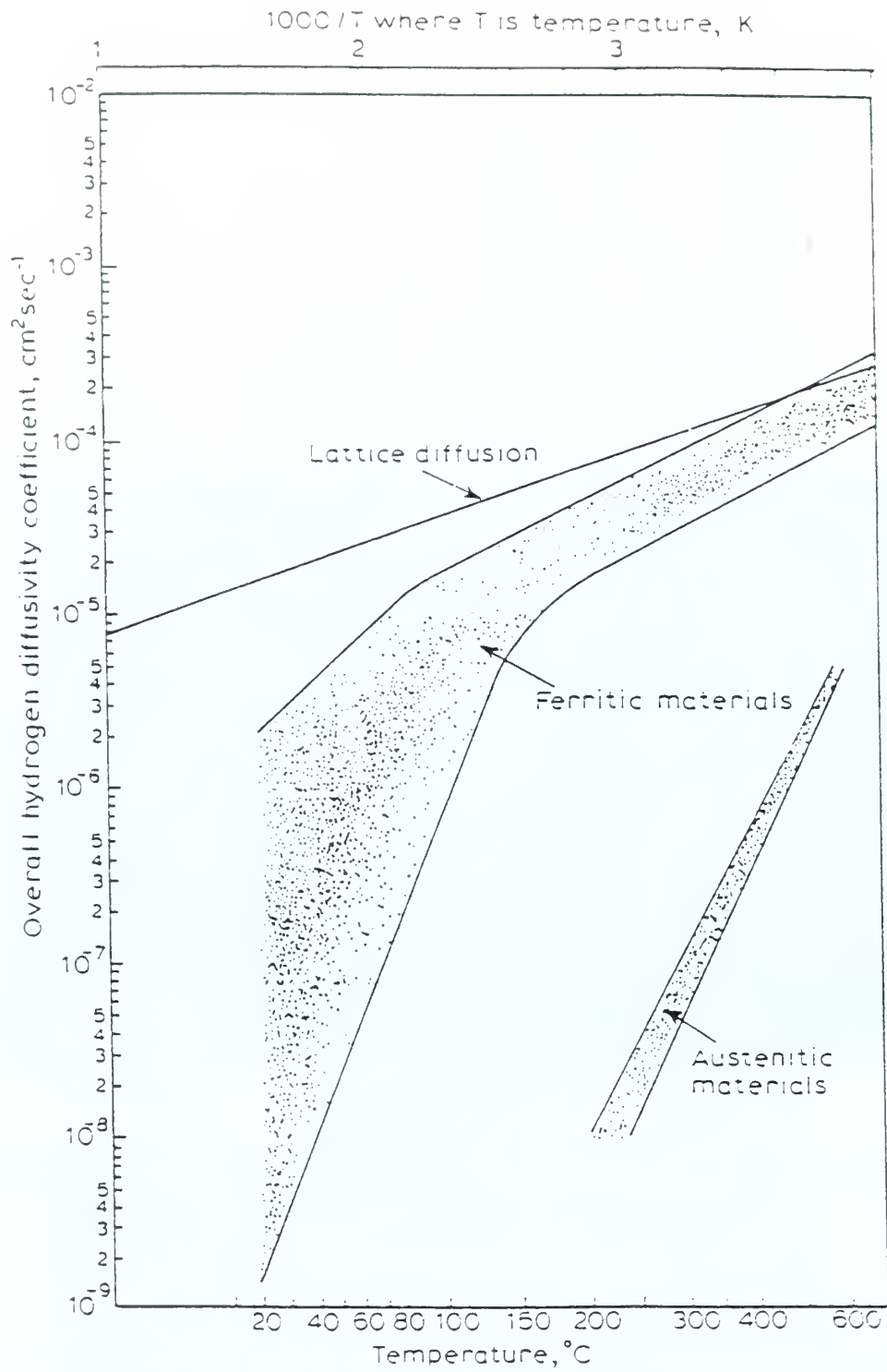
Figure 4.8 Variations in the measured diffusivities of hydrogen in ferritic and austenitic steels [Ref. 10]

V. CONCLUSIONS

As was found in previous research [Ref. 8, 9] the amount of underbead cracking found in the underwater welds was related to the water temperature. For a weld made in 5°C water this cracking was extensive but was significantly reduced for a weld made in 25°C water. Hydrogen cracking is most likely the cause of these cracks since all elements required are present for this to occur. SEM observations of the fracture surface confirmed this as transgranular cracks and secondary cracking perpendicular to the crack surface, which are signs of hydrogen assisted cracking, were detected. Because the time to cool between 800°C and 500°C was similar in all three samples, hardness readings which correspond to a martensite/bainite microstucture in the HAZ were similar in all three samples. The inclusion information that was gathered did not support the theory that increased volume fraction of inclusions leads to hydrogen being trapped in the weld pool and thus less likelihood of cracking in the coarse grained HAZ near the fusion line [Ref. 8] All results point towards diffusible hydrogen in the coarse grain region of the HAZ being the controlling factor of underbead cracking in the underwater weld samples. The 5°C sample had extensive underbead cracking while the 25°C sample had cracks which were very fine and localized near the cap of the last weld pass. Because the diffusion rate of hydrogen in weldments held in cold water is slower than in warm water, the hydrogen may diffuse away from the coarse grain HAZ near the fusion line in warm water weldments so that cracking is less likely in these.

LIST OF REFERENCES

1. AWS Committee on Welding in Marine Construction, "Specification for Underwater Welding", *American Welding Society*, (ANSI/AWS D3.6-93), August, 1992.

2. Smallman, R.E., *Modern Physical Metallurgy*, Butterworth-Heinemann Ltd. 1992.

3. Lundin, C.D., G. Zhou and K.K. Khan, "Metallurgical Characterization of the HAZ in A516-70 and Evaluation of Fracture Toughness Specimens", *Welding Research Council Bulletin*, no. 403, Report 1, pp. 1-88, July 1995.

4. Silva, E.A., "Underwater Welding and Cutting", *Metals Handbook*, 9th Edition, vol. 6, American Society of Metals, 1983.

5. Naval Sea Systems Command, *U.S. Navy Underwater Cutting and Welding Manual*, 1 April 1989.

6. Kou, S., *Welding Metallurgy*, John Wiley and Sons, 1987.

7. Ozaki, J., J. Naiman, and K. Masubuchi, "A Study of Hydrogen Cracking in Underwater Steel Welds", *Welding Journal*, Vol. 56, No. 8, pp. 231s-237s, 1977.

8. Fox, A.G., R.L. Johnson, J.F. Dill, "Effect of Water Temperature on the Underwater Wet Weldability of ASTM A516 Grade 70 Steel", Proceedings of OMAE, pp. 2262-2267, ASME International, New York, July 1998.

9. West, T.C., W.E. Mitchell and R.I. Murray, "Effects of Water Temperature on Cracking of Wet-Welded Carbon Steel", Welding Journal, vol. 75, no. 10), pp. 51-55, 1996.

10. Easterling, K., *Introduction to the Physical Metallurgy of Welding*, Butterworths, 1983.

11. Johnson, R.L., "The Effect of Water Temperature on Underbead Cracking of Underwater Wet Weldments", Thesis, Naval Postgraduate School, September 1997.

INITIAL DISRIBUTION LIST